energies

Investigation of non-isothermal kinetics and thermodynamic parameters for the pyrolysis of different date palm parts

Emmanuel Galiwango[1,*], Ali H. Al-Marzuoqi[1,*], Abbas A. Khalil[2] and Mahdi M. Abu-Omar[3]

[1] Department of Chemical and Petroleum Engineering, United Arab Emirates University, UAE; emmag@uaeu.ac.ae
2 Department of Chemistry, United Arab Emirates University, UAE; abbask@uaeu.ac.ae
3 Department of Chemistry and Biochemistry and Biochemistry, UC Santa Barbara Santa Barbara, USA; mabuomar@ucsb.edu
* Correspondence: emmag@uaeu.ac.ae (E.G), hassana@uaeu.ac.ae (A.H.M); Tel.: +971 3713-6407 (E.G); +971 3713-4470 (A.H.M)

Supplementary Materials: The following are available online at www.mdpi.com/xxx/

Figure S1. FWO model-free kinetic model fittings of (a) L, (b) R, (c) F, and (d) M of DPWP.

Figure S2. KAS model-free kinetic model fittings of (a) L, (b) R, (c) F, and (d) M of DPWP.

Figure S3. Starink model-free kinetic model fittings of (a) L, (b) R, (c) F, and (d) M of DPWP.

Figure S4. Experimental and fitted $Z(\alpha)$ master plots of (a) L at heating rates of 10, 15, 20, and 25 °Cmin^{-1}.

Figure S5. Experimental and fitted $Z(\alpha)$ master plots of (b) R at heating rates of 10, 15, 20, and 25 °Cmin^{-1}.

Figure S6. Experimental and fitted $Z(\alpha)$ master plots of (c) F at heating rates of 10, 15, 20, and 25 °Cmin^{-1}.

Figure S7. Experimental and fitted $Z(\alpha)$ master plots of (d) M at heating rates of 10, 15, 20, and 25 °Cmin^{-1}.

Figure S8. Relationship between ln A and activation energy of (a) L, (b) R, (c) F, and (d) M samples.

Figure S9. The dependence of the experimental $g(\alpha)/g(0.5)$ on conversion, Gn represents the theoretical model of $g(\alpha)/g(0.5)$, for (a) L, (b) R (c) F and (d) M.

Table S1. The activation energies and thermodynamic parameters of L determined by three model-free methods at different iso-conversions.

Table S2. The activation energies and thermodynamic parameters of R determined by three model-free methods at different iso-conversions.

Table S3. The activation energies and thermodynamic parameters of F determined by three model-free methods at different iso-conversions.

Table S4. The activation energies and thermodynamic parameters of M determined by three model-free methods at different iso-conversions.

Table S5. The parameters of DPWP mechanism functions fitted by Popescu method

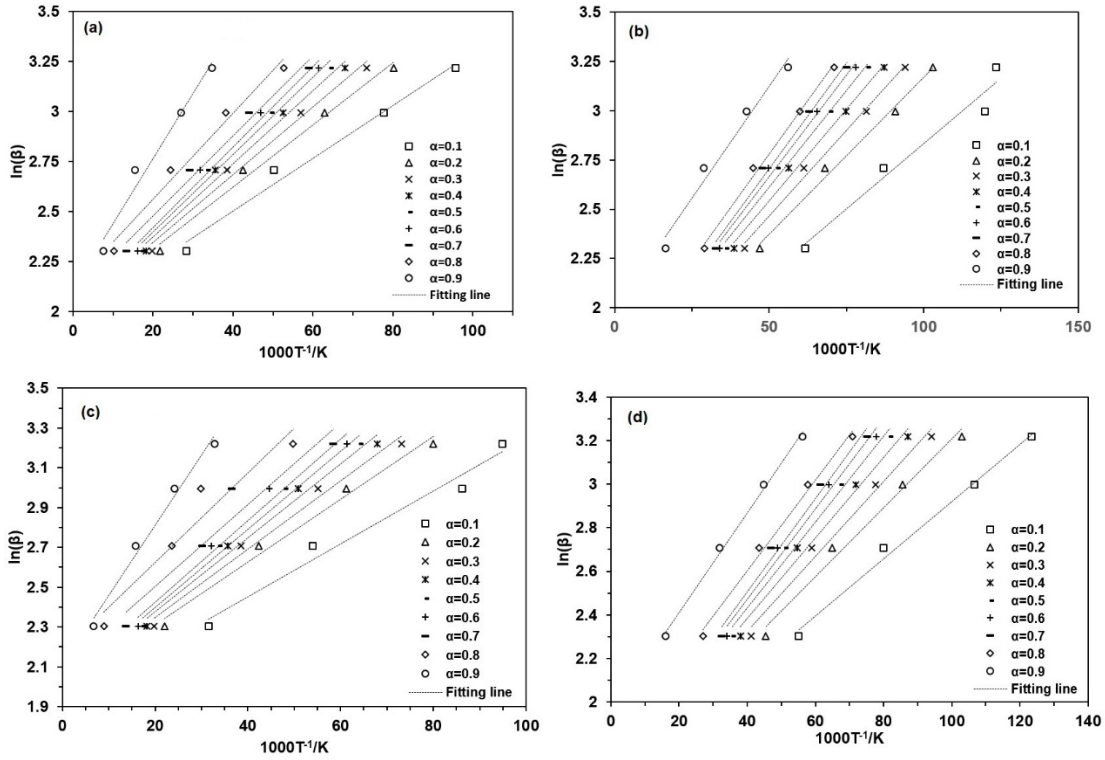


Figure S1. FWO model-free kinetic method fittings of (a) Leaflet (L), (b) Rachis (R), (c) Fiber (F), and (d) Composite (M) of DPWP.

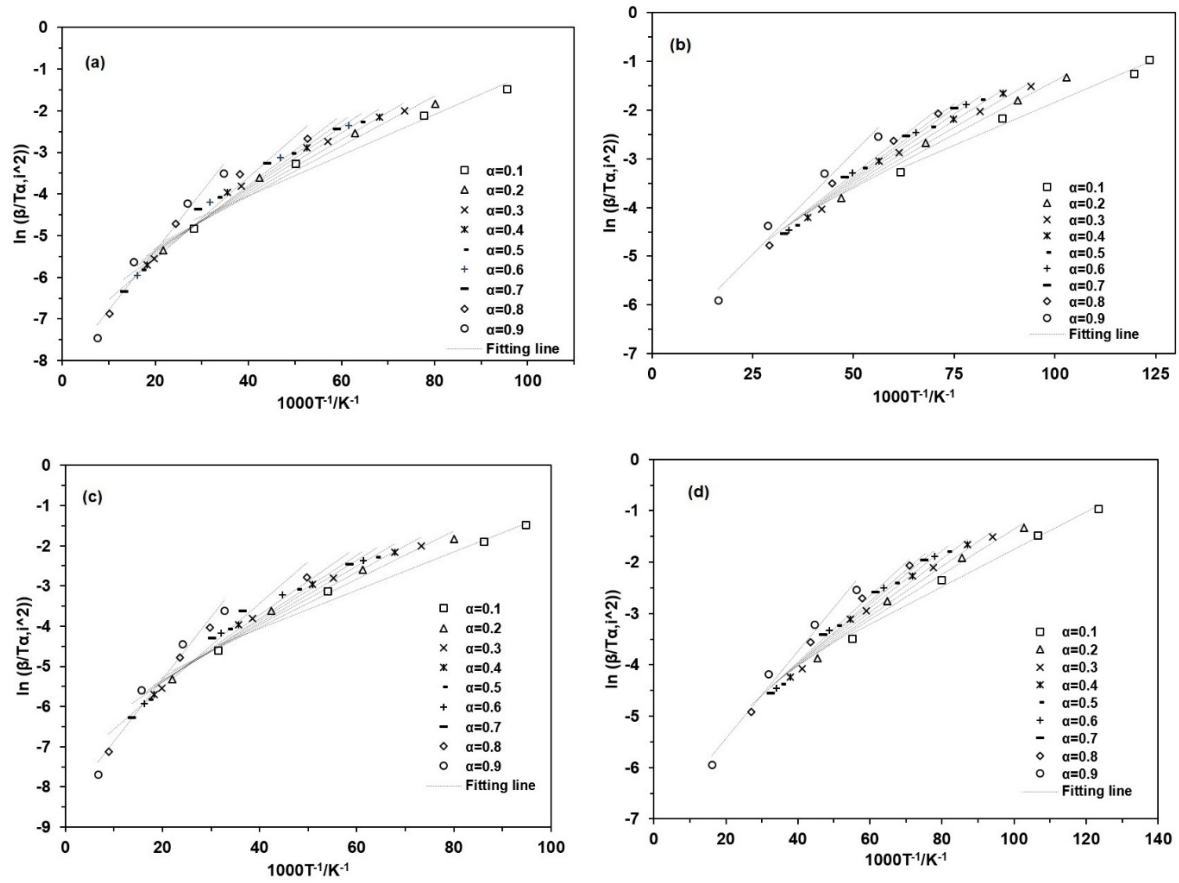


Figure S2. KAS model-free kinetic method fittings of (a) Leaflet (L), (b) Rachis (R), (c) Fiber (F), and (d) Composite (M) of DPWP.

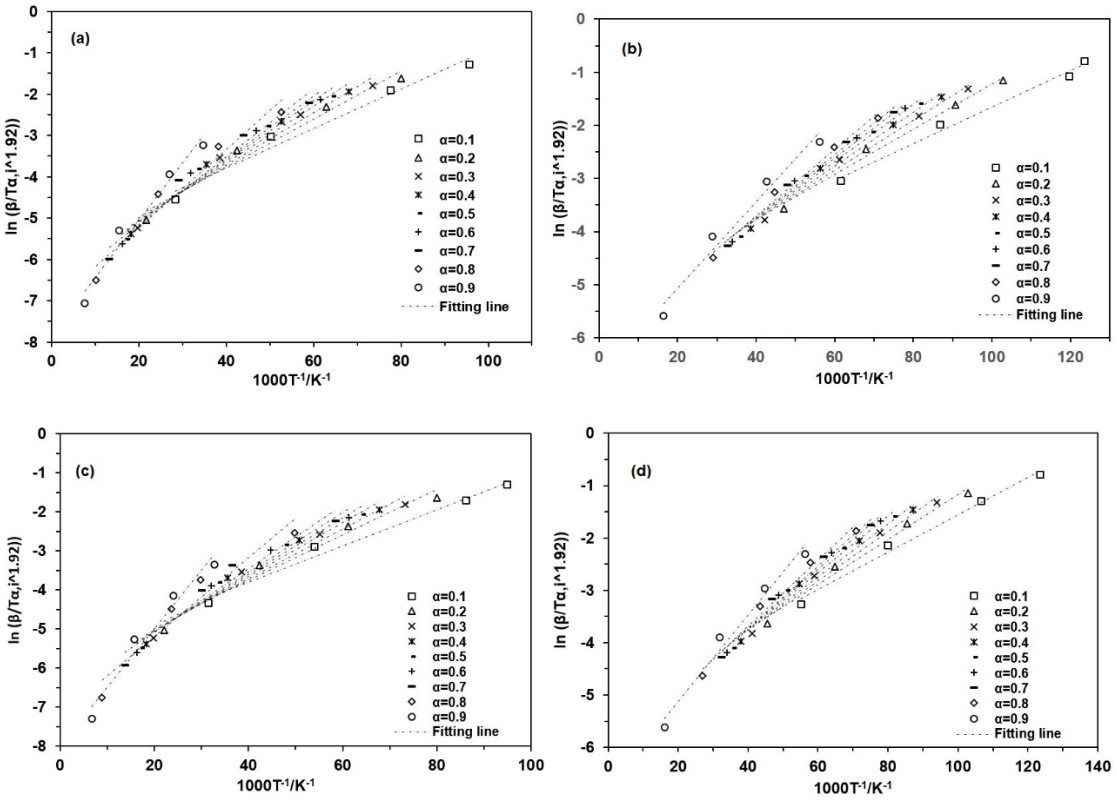


Figure S3. Starink model-free kinetic method fittings of (a) Leaflet (L), (b) Rachis (R), (c) Fiber (F), and (d) Composite (M) of DPWP.

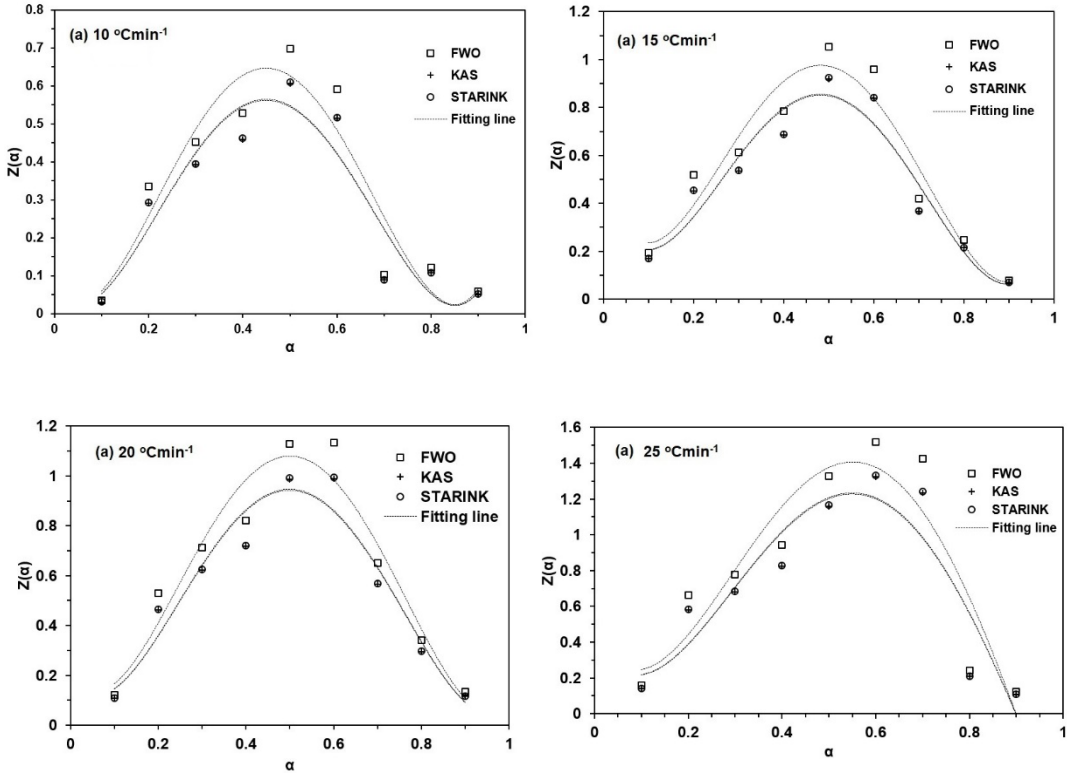


Figure S4. Experimental and fitted Z(α) master plots of (a) Leaflet (L) at heating rates of 10, 15, 20, and 25 °Cmin^{-1}.

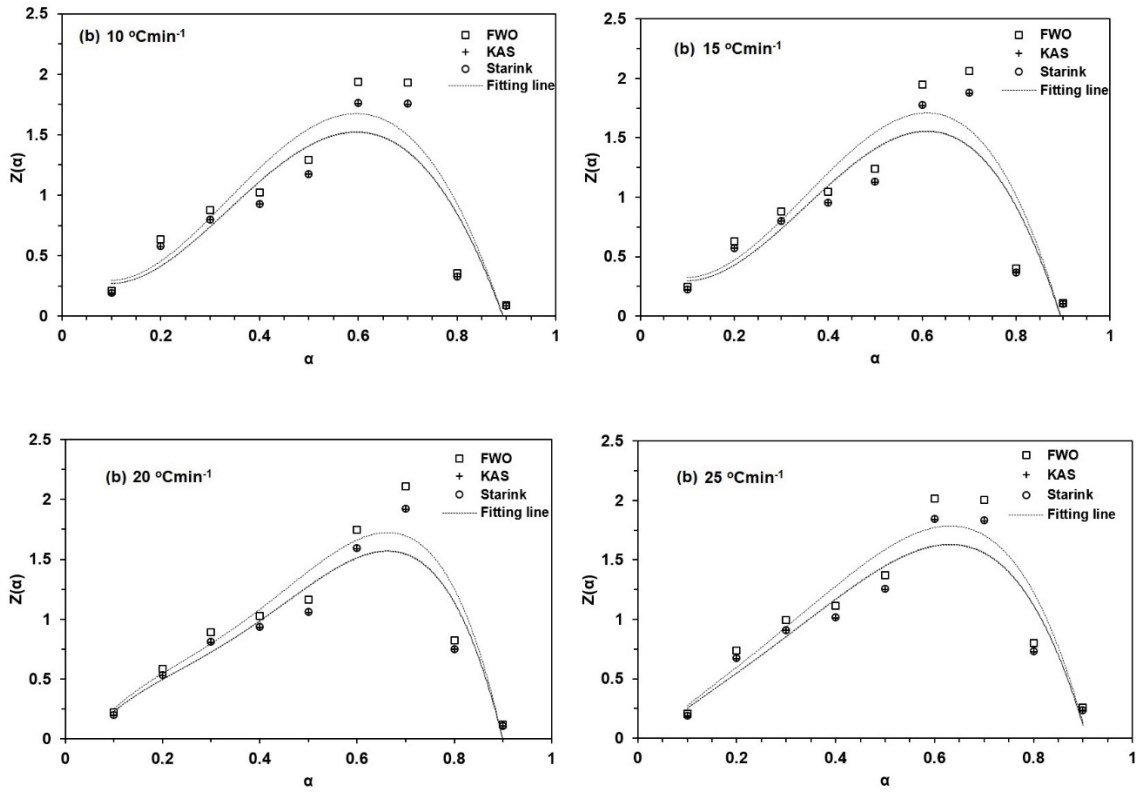


Figure S5. Experimental and fitted Z(α) master plots of (b) Rachis (R) at heating rates of 10, 15, 20, and 25 °Cmin^{-1}.

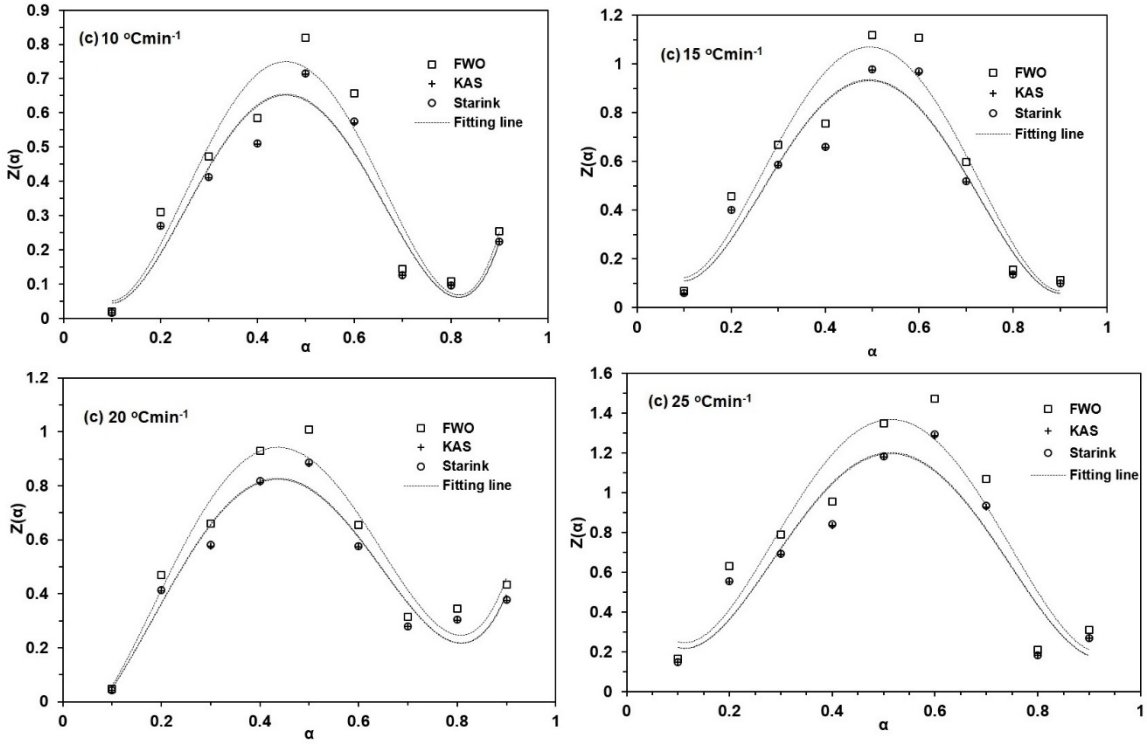


Figure S6. Experimental and fitted Z(α) master plots of (c) Fibers (F) at heating rates of 10, 15, 20, and 25 °Cmin^{-1}.

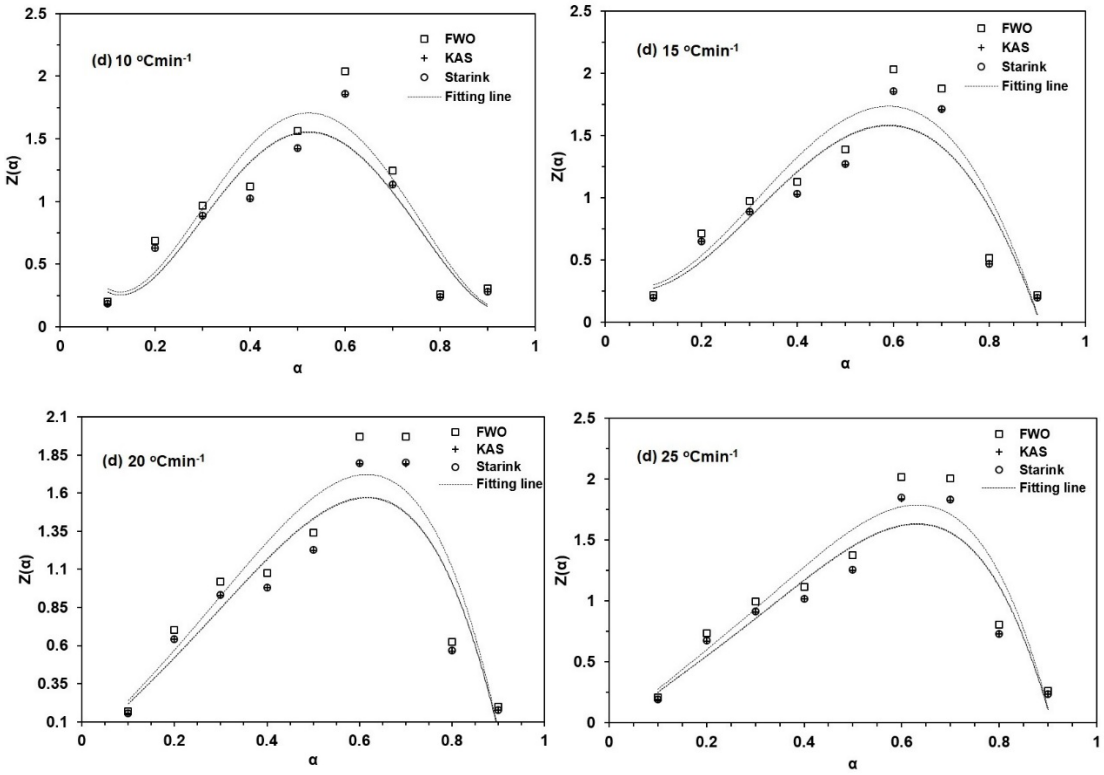


Figure S7. Experimental and fitted Z(α) master plots of (d) Composite (M) at heating rates of 10, 15, 20, and 25 °Cmin^{-1}.

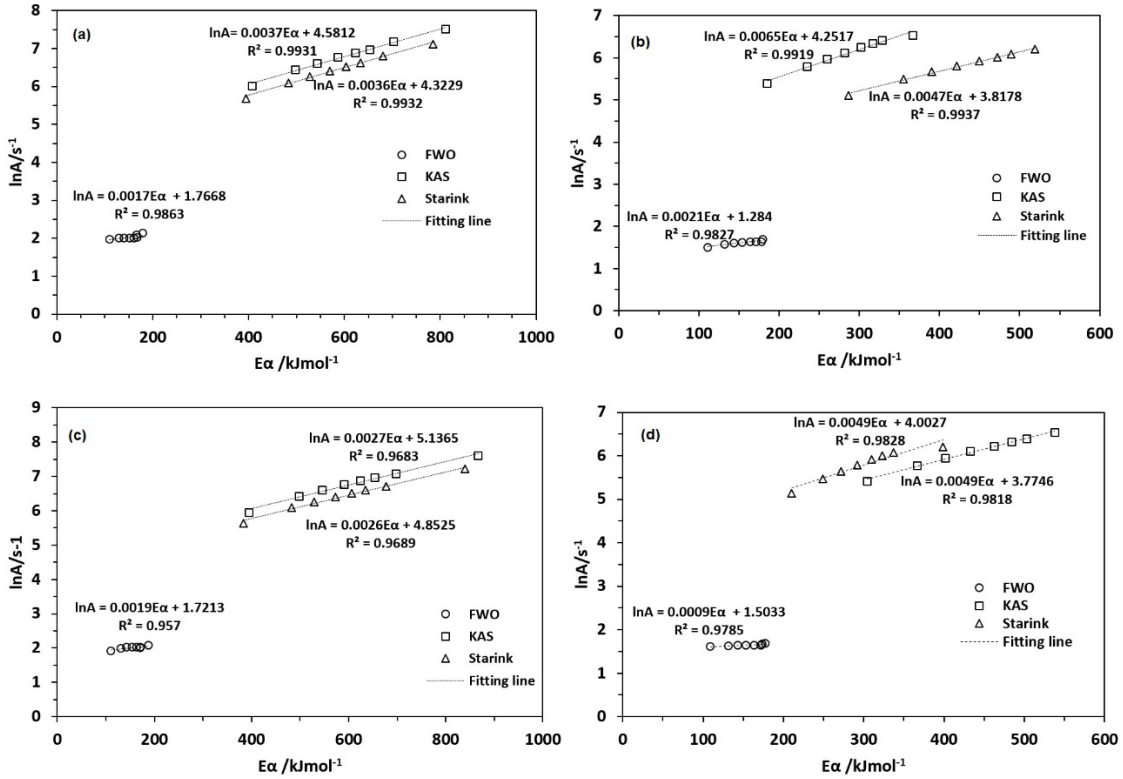


Figure S8. Relationship between lnA and activation energy of (a) Leaflet (L), (b) Rachis (R), (c) Fiber (F), and (d) Composite (M) samples.

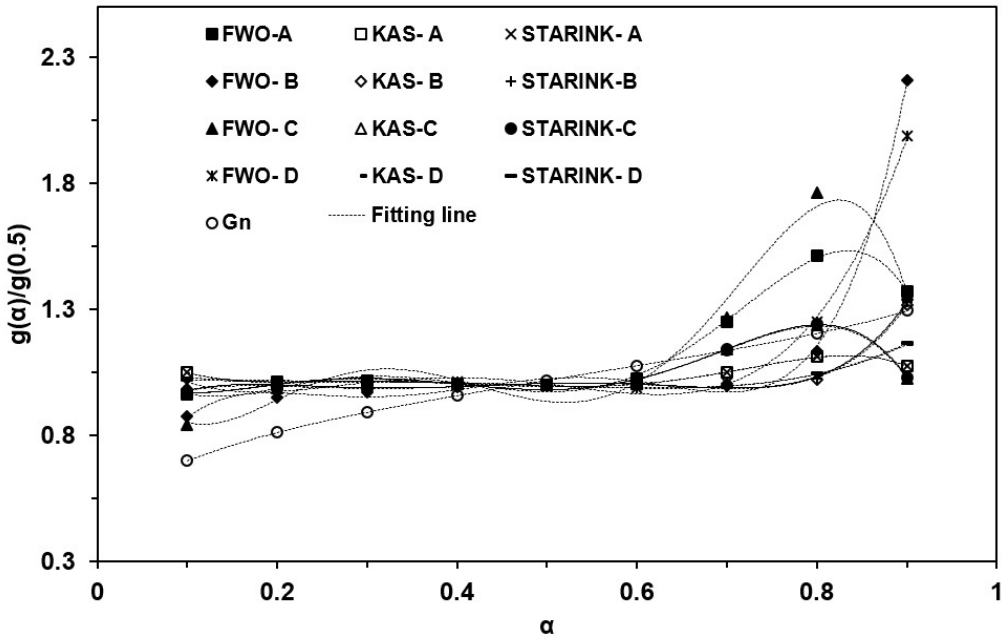


Figure S9. The dependence of the experimental g(α)/g(0.5) on conversion, Gn represents the theoretical model of g(α)/g(0.5), for (a) Leaflet (L), (b) Rachis (R), (c) Fiber (F), and (d) Composite (M).

Table S1. The activation energies and thermodynamic parameters of L determined by three model-free methods at different iso-conversions.

	FWO- Leaflet (L)				**KAS- Leaflet (L)**				**Starink- Leaflet (L)**			
α	E_α /kJmol^{-1}	Log A (s^{-1})	ΔG/kJ mol^{-1}	ΔS/ $Jmol^{-1}$	E_α /kJmol^{-1}	Log A (s^{-1})	ΔG/kJ mol^{-1}	ΔS/ Jmol^{-1}	E_α /kJmol^{-1}	Log A (s^{-1})	ΔG/kJ mol^{-1}	ΔS /$Jmol^{-1}$
0.1	109.74	11.75	149.97	−0.091	407.39	45.07	144.65	0.531	394.92	43.67	144.78	0.505
0.2	129.70	12.69	163.90	−0.073	498.01	49.67	157.95	0.632	483.04	48.17	158.08	0.603
0.3	140.51	13.16	171.40	−0.064	543.74	51.89	165.16	0.674	527.94	50.38	165.29	0.645
0.4	152.15	13.72	178.21	−0.054	586.97	53.94	171.74	0.712	569.51	52.33	171.88	0.681
0.5	161.29	14.12	183.80	−0.046	622.72	55.54	177.13	0.742	603.60	53.83	177.28	0.709
0.6	167.11	14.23	188.99	−0.044	652.65	56.54	182.08	0.763	633.53	54.88	182.23	0.731
0.7	166.28	13.56	200.05	−0.061	702.53	58.48	192.34	0.786	680.92	56.68	192.51	0.752
0.8	178.75	13.52	222.67	−0.069	810.62	63.24	213.74	0.835	785.67	61.29	213.92	0.800
0.9	270.21	16.14	284.92	−0.024	1183.0	72.83	273.84	1.002	1146.50	70.56	274.07	0.961

R^2 were above 0.98

Table S2. The activation energies and thermodynamic parameters of R determined by three model-free methods at different iso-conversions.

	FWO- Rachis (R)				**KAS- Rachis (R)**				**Starink- Rachis (R)**			
α	E_α /kJmol^{-1}	Log A (s^{-1})	ΔG/kJ mol^{-1}	ΔS/ Jmol^{-1}	E_α /kJmol^{-1}	Log A (s^{-1})	ΔG/kJ mol^{-1}	ΔS/ Jmol^{-1}	E_α /kJmol^{-1}	Log A (s^{-1})	ΔG/kJ mol^{-1}	ΔS /Jmol^{-1}
0.1	110.58	27.57	55.39	0.220	294.32	72.38	53.81	1.078	286.83	70.57	53.85	1.043
0.2	132.19	27.67	70.03	0.220	364.98	75.46	67.98	1.135	355.01	73.42	68.03	1.096
0.3	143.83	27.60	77.47	0.218	400.73	76.02	75.19	1.145	389.93	73.99	75.25	1.106
0.4	153.81	27.44	84.03	0.215	432.33	76.29	81.55	1.150	421.52	74.41	81.61	1.114
0.5	163.79	27.44	90.22	0.214	461.43	76.51	87.57	1.154	449.79	74.60	87.63	1.117
0.6	171.27	27.40	95.05	0.213	484.71	76.79	92.25	1.158	472.24	74.83	92.32	1.121
0.7	177.92	27.46	98.75	0.214	503.00	76.89	95.84	1.160	489.69	74.87	95.92	1.121
0.8	179.58	26.23	106.41	0.190	532.93	77.13	103.15	1.164	518.79	75.10	103.23	1.125
0.9	188.73	21.93	161.39	0.106	696.71	80.36	155.65	1.224	675.93	77.98	155.78	1.179

R^2 were above 0.98

Table S3. The activation energies and thermodynamic parameters of F determined by three model-free methods at different iso-conversions.

	FWO- Fibers (F)				**KAS- Fibers (F)**				**Starink- Fibers (F)**			
α	E_α /kJmol^{-1}	Log A (s^{-1})	ΔG/kJ mol^{-1}	ΔS/ $Jmol^{-1}$	E_α /kJmol^{-1}	Log A (s^{-1})	ΔG/kJ mol^{-1}	ΔS/ $Jmol^{-1}$	E_α /kJmol^{-1}	Log A (s^{-1})	ΔG/kJ mol^{-1}	ΔS /$Jmol^{-1}$
0.1	110.58	32.37	57.00	0.264	394.92	116.10	62.57	1.448	383.28	112.68	62.62	1.397
0.2	131.36	27.71	74.58	0.213	498.01	105.78	73.84	1.578	483.04	102.60	73.91	1.522
0.3	143.00	27.39	82.18	0.208	546.23	105.27	80.62	1.594	529.60	102.06	80.70	1.537
0.4	153.81	27.28	88.94	0.205	590.29	105.33	87.00	1.603	572.83	102.21	87.08	1.547
0.5	162.95	27.35	94.23	0.206	624.38	105.52	92.08	1.607	606.09	102.43	92.16	1.552
0.6	170.44	27.22	99.47	0.202	654.31	105.09	96.27	1.616	635.19	102.02	96.35	1.560
0.7	171.27	25.46	112.99	0.148	697.54	104.41	100.97	1.650	676.76	101.30	101.06	1.592
0.8	187.07	23.22	148.57	0.077	867.15	108.59	118.57	1.777	839.71	105.16	118.68	1.711
0.9	291.82	24.17	205.84	0.123	1288.7	107.65	181.72	1.755	1248.8	104.31	181.89	1.691

R^2 were above 0.98

Table S4. The activation energies and thermodynamic parameters of M determined by three model-free methods at different iso-conversions.

	FWO- Composite **(M)**				**KAS-** Composite **(M)**				**Starink-** Composite **(M)**			
α	E_α /kJmol^{-1}	Log A (s^{-1})	ΔG/kJ mol^{-1}	ΔS/ $Jmol^{-1}$	E_α /kJmol^{-1}	Log A (s^{-1})	ΔG/kJ mol^{-1}	ΔS/ $Jmol^{-1}$	E_α /kJmol^{-1}	Log A (s^{-1})	ΔG/kJ mol^{-1}	ΔS /$Jmol^{-1}$
0.1	108.91	11.79	148.12	−0.090	304.29	33.46	143.99	0.324	296.81	23.10	145.47	0.126
0.2	131.36	13.06	161.34	−0.065	366.65	36.94	156.86	0.391	357.50	25.03	158.55	0.164
0.3	143.00	13.62	168.64	−0.055	401.57	38.73	163.94	0.425	390.76	26.16	165.72	0.185
0.4	152.98	14.04	175.23	−0.047	433.16	40.23	170.31	0.454	421.52	27.11	172.17	0.203
0.5	163.79	14.54	181.19	−0.038	462.26	41.55	176.12	0.479	449.79	27.83	178.07	0.216
0.6	172.10	14.92	185.66	−0.031	484.71	42.55	180.48	0.497	472.24	28.29	182.51	0.225
0.7	177.09	15.04	189.73	−0.029	503.00	43.22	184.40	0.510	489.69	28.92	186.45	0.237
0.8	173.76	14.14	200.52	−0.050	537.92	44.46	194.45	0.524	522.95	32.94	196.06	0.306
0.9	190.39	13.27	248.25	-0.079	707.52	50.64	239.64	0.594	686.74	46.46	240.21	0.519

R^2 were above 0.98

Table S5. The parameters of DPWP mechanism functions fitted by Popescu method

	Leaflet (L)		**Rachis (R)**		**Fiber (F)**		**Composite (M)**	
Model								
	I	R^2	**I**	R^2	**I**	R^2	**I**	R^2
FWO	0.003	0.9927	0.0025	0.9998	0.0032	0.9928	0.0022	0.9991
KAS	0.0044	0.9553	0.0272	0.9992	0.0386	0.9907	0.0272	0.9936
STARINK	0.0331	0.9869	0.0252	0.9992	0.0357	0.9913	0.0053	0.999

Publisher's Note: MDPI stays neutral with regard to jurisdictional claims in published maps and institutional affiliations.

© 2020 by the authors. Licensee MDPI, Basel, Switzerland. This article is an open access article distributed under the terms and conditions of the Creative Commons Attribution (CC BY) license (http://creativecommons.org/licenses/by/4.0/).